
SH.A. MIRSAGATOV,¹ B.N. ZAVERYUKHIN,¹ O.K. ATABOEV,²
N.N. ZAVERYUKHINA¹

¹ Physical and Technical Institute, Scientific Production Association “Physics–Sun”,
Uzbek Academy of Sciences

(2b, Bodomzor Str., Tashkent 100084, Uzbekistan; e-mail: mirsagatov@uzsci.net)

² Berdakh Karakalpak State University

(1, Ch. Abdirrov Str., Nukus 230113, Republic Karakalpakistan; e-mail: omonboy12@uzsci.net)

CASCADE INJECTION PHOTODETECTOR FOR THE 500–650-nm SPECTRAL RANGE ON THE BASIS OF SOLID SOLUTIONS OF A²B⁶ COMPOUNDS

PACS 07.60.-j, 78.55.Et

The parameters of film injection photodetectors (FIPDs) created on the basis of solid solutions of A²B⁶ compounds for a spectral range of 500–650 nm have been studied. The sensitive region of FIPDs is formed as a sandwich from films with different composition contents and different energy gap widths. The mechanism of FIPD functioning is based on the selective absorption of radiation by films and its conversion into an electric signal. FIPDs are characterized by an internal enhancement of a photocurrent and can efficiently register weak optical signals at illuminances $E \leq 1$ lux and the temperature $T = 300$ K. The integral sensitivity of FIPDs is $S_{\text{int}} \approx 75$ A/lm ($\approx 8 \times 10^3$ A/W).

Keywords: injection photodetector, photocurrent, Schottky barrier.

1. Introduction

Semiconductor-based photodetectors with injection enhancement of the initial photocurrent, which are composed of different materials, represent a new class of photodetectors. They have been studied well enough in both experimental and theoretical aspects. The mechanism of functioning of those photodetectors was described in a recent review devoted to injection photodetectors [1]. The researches were carried out for single-crystalline (Ge, Si) injection photodetectors (IPDs). They are the most sensitive in the infra-red spectral range.

Injection photodetectors on the basis of wide-gap A³B⁵ compounds were also developed and studied. They are characterized by excellent operational parameters in the spectral interval $\lambda \approx 0.3 \div 0.8$ μm [1]. Their current sensitivity reaches the maximum

$S = 500$ A/W at the wavelength $\lambda \approx 0.8$ μm . However, all mentioned IPDs have a common and very substantial shortcoming: nitrogen temperatures are required for them to work effectively.

As was marked in work [1], IPDs on the basis of A²B⁶ compounds (ZnS and CdS single crystals) are rather promising for the registration and the analysis of radiation in the ultra-violet and visible spectral ranges. Those IPDs have an integral current sensitivity of 0.2–1.5 A/W at $\lambda = 0.3$ μm . An advantage of single-crystalline IPDs on the basis of A²B⁶ compounds in comparison with IPDs fabricated from other materials is their better parameters at room temperature.

Among the works devoted to IPDs, we know only one dealing with an IPD with internal current enhancement, which was created on the basis of a *p*-CdTe film [2]. This film IPD effectively works in a narrow spectral interval. The current sensitivity of CdTe-IPD amounts to $S \approx 2.6$ A/W at $\lambda \approx 0.625$ μm

© SH.A. MIRSAGATOV, B.N. ZAVERYUKHIN,
O.K. ATABOEV, N.N. ZAVERYUKHINA, 2013

ISSN 2071-0194. Ukr. J. Phys. 2013. Vol. 58, No. 5

and the temperature $T = 300$ K, which is approximately 5 to 6 times worse than the corresponding parameter for an ideal photodetector at the same wavelength λ [3]. By the ideal photodetector, we mean a photodetector, in which all incident quanta of electromagnetic radiation are absorbed, and all generated electron-hole pairs are separated by the barrier without losses, thus contributing to the photocurrent. For such a photodetector, the current sensitivity at a given wavelength is calculated by the formula $S = e\lambda/hc$, where e is the electron charge, h Planck's constant, c the light velocity, and λ the wavelength of electromagnetic radiation, and does not depend on the specific material.

A film p -CdTe-based IPD is a metal–semiconductor–metal (MSM) structure with a Schottky barrier injecting the minority charge carriers into the base depth. This IPD effectively works at a forward bias voltage and the temperature $T = 300$ K. The p -CdTe film is a sensitive element of IPD. However, this detector has a narrow spectral interval of effectively registered electromagnetic radiation in the visible range of the spectrum, $\lambda \approx 0.62 \div 0.65 \mu\text{m}$.

It should be noted that the interval of the high photodetector sensitivity to a weak optical illumination of 0.05–1.0 lux is confined to that of intrinsic photosensitivity in the material (CdTe), from which the p -CdTe-based IPD is fabricated. Hence, it follows that, for extremely weak optical signals to be detected in a wider interval of the visible spectral range from ultra-violet to infra-red wavelengths, a set of semiconducting materials with different energy gaps should be used. Therefore, it becomes evident from the aforesaid that there exists a difficulty in the creation of IPDs that would possess a high sensitivity to weak optical illumination in a wide visible spectral range and work at room temperature.

In the framework of this problem, we pose a task to create a cascade injection photodetector (CIPD) with internal current enhancement on the basis of A^2B^6 -compound films. Its structure had to be of the sandwich type, i.e. it had to include layers of different A^2B^6 compounds. As a result, this CIPD should effectively register weak optical signals (at the illuminances $E \geq 0.5$ lux) at $T = 300$ K in a wider wavelength interval, $\lambda \approx 0.5 \div 0.65 \mu\text{m}$, in comparison with single-crystalline and film IPDs on the basis of A^2B^6 compounds.

2. Cascade Injection Photodetector on the Basis of A^2B^6 Compounds

The lack of data concerning injection photodetectors on the basis of A^2B^6 compounds is associated with difficulties in obtaining the conductivity of the p -type in those materials (cadmium and zinc tellurides are exceptions), as well as small diffusion shift lengths for the minority charge carriers in them. In order to create effective injection photodiodes on the basis of semiconducting A^2B^6 compounds, either materials with improved properties such as in work [2] or layers of solid solutions with different composition contents have to be synthesized. We selected the latter way. In order to create an injection photodetector with enhanced photosensitivity in the wavelength interval $\lambda = 500 \div 670$ nm, we used such solid solutions as n -CdS $_x$ Te $_{1-x}$ with high specific resistivities and p -Cd $_x$ Zn $_{1-x}$. Detectors of electromagnetic radiation with indicated properties are intended to be used in optical spectral analyzers, e.g., for the analysis of chemical elements in metallic alloys that emit electromagnetic waves in this range [3].

The injection photodetector was created as follows. By the method of sublimation in a hydrogen flux, a polycrystalline large-domain p -CdTe film (a layer) was grown on the surface of a molybdenic (Mo) wafer of the thickness $d = 300 \mu\text{m}$, which played the role of substrate and rear electric contact (the cathode). The specific resistance of the film $\rho = 10^2 \div 10^3 \Omega \cdot \text{cm}$, and its thickness $d = 2.8 \mu\text{m}$. Then the following layers were grown one by one on the surface of p -CdTe films with the use of the method of gas-transport epitaxy in the hydrogen flux:

(i) a p -Cd $_x$ Zn $_{1-x}$ Te film (a layer of polycrystalline large-domain solid solutions, $0.516 < x < 0.693$) with the specific resistance $\rho \approx 10^3 \div 10^4 \Omega \cdot \text{cm}$ and the thickness $d = 20 \mu\text{m}$;

(ii) an i -CdS $_x$ Te $_{1-x}$ film (a layer of almost the i -type of conductivity, $0.77 < x < 0.93$) with the specific resistance $\rho \approx 10^8 \div 10^9 \Omega \cdot \text{cm}$ and the thickness $d = 2.5 \mu\text{m}$.

Afterward, by sputtering cadmium sulfide (CdS) in vacuum ($P \approx 10^{-5}$ Torr), the surface of the i -CdS $_x$ Te $_{1-x}$ film was covered with an n -CdS film (a layer) with the specific resistance $\rho \approx 1.0 \Omega \cdot \text{cm}$ and the thickness $d = 1 \div 2 \mu\text{m}$. A Π -shaped electric contact (the anode) of the thickness $d = 550 \text{ \AA}$ was formed on the surface of the n -CdS film using the

method of vacuum evaporation of indium (In). The n -CdS film played the role of input window for electromagnetic radiation.

In such a way, we created a photosensitive In- n -CdS- i -CdS $_x$ Te $_{1-x}$ - p -Cd $_x$ Zn $_{1-x}$ Te- p -CdTe-Mo structure with the active area of the input window $S = 0.5 \text{ cm}^2$. In total, 25 photodetectors with similar electrophysical and spectral characteristics were fabricated and researched.

The injection photodetector fabricated on the basis of this structure has a sensitive region composed of semiconducting films (layers) with metallic contacts attached to the upper and lower films. The photosensitivities of those layers to electromagnetic radiation are different in the far-ultraviolet, visible, and near infra-red spectral ranges. The fabricated IPD differs from the available analogs in that its sensitive region is made of A²B⁶ semiconductor (CdS) with the electron (n) type of conductivity, a semiconducting solid solution CdS $_x$ Te $_{1-x}$ with the intrinsic (i) type of conductivity, a semiconducting solid solution Cd $_x$ Zn $_{1-x}$ Te with the hole (p) type of conductivity, and A²B⁶ semiconductor CdTe with the hole type of conductivity. The described injection photodetector has also the following specific features of its design:

(i) the sensitive region consists of four semiconducting films (CdS, CdS $_x$ Te $_{1-x}$, Cd $_x$ Zn $_{1-x}$ Te, and CdTe layers) with different specific resistances arranged like a sandwich; i.e. this is a cascade structure;

(ii) the upper film is a CdS layer, and the lower one is a p -CdTe layer;

(iii) between the upper n -CdS and lower p -CdTe films, there is an i -CdS $_x$ Te $_{1-x}$ film playing the role of IPD base; in the space between the upper and lower films, there is also a p -Cd $_x$ Zn $_{1-x}$ Te film, playing the role of transient element between the base and the p -CdTe film; this film serves for an optimum decrease of the potential barrier to provide an almost "barrier-free" transition of charge carriers; the base has the intrinsic type of conductivity (i) and the largest specific resistance among all semiconducting films;

(iv) the front electric contact is attached to the upper semiconducting film (n -CdS), and the rear electric contact to the lower semiconducting film (p -CdTe);

(v) the n -CdS film plays the role of input window for registered electromagnetic radiation.

Hence, the sensitive region of a cascade injection photodetector (CIPD) is an $n-i-p$ structure with $i-p$ base.

3. Electrophysical and Photoelectric Characteristics of Cascade Injection Photodetector on the Basis of A²B⁶ Compounds

3.1. Current-voltage characteristic of the cascade injection photodetector

The created $n-i-p$ structure possesses rectification capabilities, as one can see from its current-voltage characteristic (CVC) depicted in Fig. 1. The rectification factor K determined as a ratio between the forward and reverse currents, $K = I_{\text{forward}}/I_{\text{reverse}}$, at the fixed voltage $V = 5 \text{ V}$ is higher than a thousand. The current in the structure is assumed to run in the forward direction if a positive potential is applied to the Mo contact and in the reverse one if the bias voltage on this contact is negative, $V_b < 0$.

3.2. Spectral distribution of the photo-emf of the cascade injection photodetector

In Fig. 2, the spectral distribution of the photo-emf, V_{emf} , of the In- n -CdS- i -CdS $_x$ Te $_{1-x}$ - p -Cd $_x$ Zn $_{1-x}$ Te- p -CdTe-Mo structure at $V_b = 0 \text{ V}$ is depicted in relative units. The figure demonstrates that the curve describing the spectral distribution of the CIPD photosensitivity consists of two sections. In the first section ($\lambda \approx 500 \div 640 \text{ nm}$, see Fig. 2, *a*), the dependence of $V_{\text{emf}}/V_{\text{emf,max}}$ on λ is growing and reaches a maximum in the second section at $\lambda \approx 630 \text{ nm}$. Then, it drastically decreases and reaches the minimum value at $\lambda \approx 660 \text{ nm}$. It should be noted that, in certain

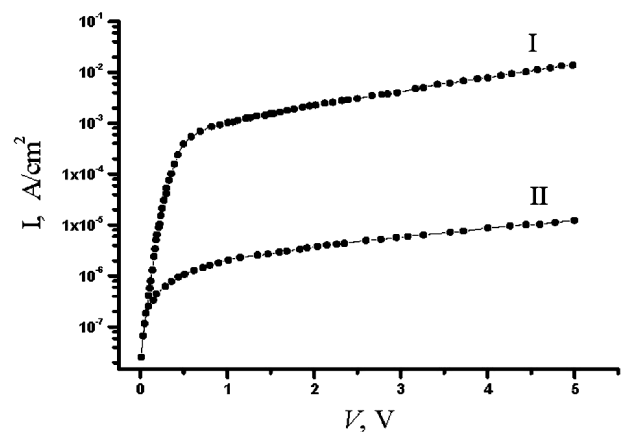


Fig. 1. Forward (I) and reverse (II) branches of dark CVC of the typical In- n -CdS- i -CdS $_x$ Te $_{1-x}$ - p -Cd $_x$ Zn $_{1-x}$ Te- p -CdTe-Mo structure at room temperature

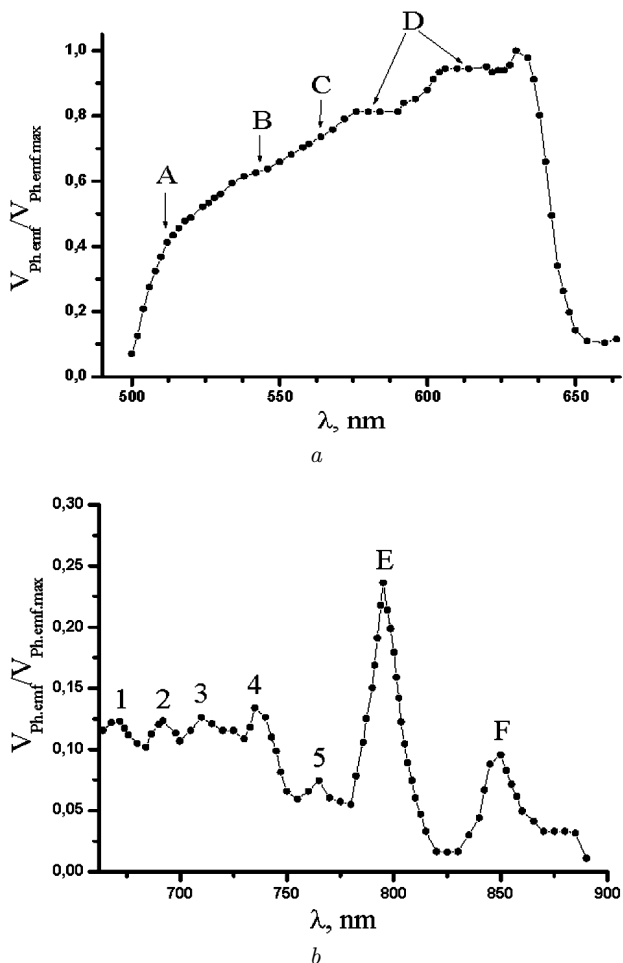


Fig. 2. First (a) and second (b) sections in the spectral distribution of the photosensitivity of the typical In-*n*-CdS-*i*-CdS_{*x*}Te_{1-*x*}-*p*-Cd_{*x*}Zn_{1-*x*}Te-*p*-CdTe-Mo structure at room temperature, $V_b = 0$ V

wavelength intervals, this curve reveals some features of its growth, such as bending points A, B, and C and plateau D.

For the interpretation of experimental data obtained for the dependence $V_{\text{emf}}/V_{\text{emf.max}} = f(\lambda)$, it is worth selecting those wavelength intervals, where this dependence demonstrates the features in its behavior. The exhibited spectral distribution of the photo-emf was measured for the cascade injection photodetector at the bias voltage $V_b = 0$ V. Various features observed in the experimental data for the growth of the CIPD photosensitivity in different wavelength intervals can be explained proceeding from the theory of optical semiconductor properties [4].

The phenomenological and theoretical considerations show that the absorption efficiency of electromagnetic radiation quanta by semiconductors depends on the energy of quanta, the band structure of semiconductors, and the action of external physical fields [4, 5]. Having separated and analyzed the wavelength intervals, we estimated the energy gap widths, E_g , for the layers of A²B⁶ compounds in the photodetector structure and the limits of their energy localization. The nature of those layers was also specified. As a result, we may conclude that the following factors are responsible for the emergence of features in the dependence $V_{\text{emf}}/V_{\text{emf.max}} = f(\lambda)$.

(i) The *n*-CdS layer with the energy gap width $E_{1g} \approx 2.48 \div 2.43$ eV (the difference $\Delta E_{1g} = 0.05$ eV) governs the dependence concerned in the first wavelength interval.

(ii) The layer of solid solution *i*-CdS_{*x*}Te_{1-*x*} with the energy gap width $E_{2g} \approx 2.43 \div 1.968$ eV ($\Delta E_{2g} = 0.462$ eV) plays the crucial role in the other intervals. This energy gap is associated with the presence of intermediate CdS_{*x*}Te_{1-*x*} sublayers with different *x* contents and, respectively, with different energy gap widths. These intermediate sublayers manifest themselves on the curve of the spectral distribution of the photosensitivity as plateaux.

Bendings A, B, and C (Fig. 2, a) in the dependence $V_{\text{emf}}/V_{\text{emf.max}} = f(\lambda)$ testify in favor of smooth transitions between the A²B⁶ layers. Bending A corresponds to the transition from the CdS layer to the CdS_{*x*}Te_{1-*x*} one, and bendings B and C to smooth transitions from one intermediate layer to the next. All those intermediate layers have different composition contents and energy gap widths. The smooth character of bending points testifies that there is no drastic interface between layers and interlayers, and the lattice constants in all layers and sublayers are almost identical. Two plateaux D, on the contrary, correspond to drastic transitions between intermediate layers. A rapid recession of the photoconductivity in the eighth section in the interval $\lambda \approx 630 \div 660$ nm evidences the existence of a weakly photoactive interlayer between the CdS_{*x*}Te_{1-*x*} layer and the layer of solid solution Cd_{*x*}Zn_{1-*x*}Te. This recession may be associated with the effect of optical quenching of the photoconduction at $\lambda \approx 630 \div 660$ nm that arises owing to the optical recharge of local centers in the interlayer [6] or to the modulations of this interlayer resistance,

which are not so large as the modulation of the base resistance.

The solid solution $\text{Cd}_x\text{Zn}_{1-x}\text{Te}$ is responsible for the peculiarities observed in the dependence $V_{\text{emf}}/V_{\text{emf.max}} = f(\lambda)$ in the interval $\lambda \approx 660 \div 780$ nm of the eighth wavelength section. Those features are well observed as five peaks at the wavelengths $\lambda = 672, 692, 710, 735,$ and 765 nm (Fig. 2, *b*, curves 1 to 5, respectively). We may assert that those peaks stem from the existence of five weakly photoactive interlayers of the solid solution $\text{Cd}_x\text{Zn}_{1-x}\text{Te}$, which are adjacent to the *p*-CdTe layer surface. The following processes take place in those intermediate layers of solid solution $\text{Cd}_x\text{Zn}_{1-x}\text{Te}$:

(i) the resistances of those layers are weakly modulated;

(ii) nonequilibrium charge carriers are optically generated by the quanta with energy in the range $E_f = 1.845 \div 1.589$ eV.

The ninth wavelength section ($\lambda \approx 780 \div 884$ nm) contains two peaks, E and F, which are related to the hexagonal and cubic modifications of cadmium telluride with the energy gap widths $E_g(\text{CdTe}^1) \approx 1.53$ eV and $E_g(\text{CdTe}^2) \approx 1.43$ eV, respectively, at $T = 300$ K [7]. This statement is confirmed by the close values of energy gaps, $E_g(\text{CdTe}^1) \approx 1.503$ eV and $E_g(\text{CdTe}^2) \approx 1.415$ eV, for the *p*-CdTe layer determined by us by extrapolating the long-wave sides of peaks E and F to the λ -axis.

3.3. Capacitance-voltage characteristic of the cascade injection photodetector

The capacitance-voltage characteristic $C(V)$ of CIPD contains four well-pronounced plateaux in the interval of reverse bias voltages, at which the thickness of the space charge layer broadens. This fact testifies that the base region of the structure is inhomogeneous and contains intermediate layers of solid solution $\text{CdS}_x\text{Te}_{1-x}$, as was discussed in Section 3.2. Moreover, the presence of cusps and plateaux in the negative branch of the $C(V)$ dependence at $V_b = -0.5 \div -2.5$ V (Fig. 3) evidences the existence of the thin (narrower than one micron) layer of an inhomogeneous insulator (oxides) in the studied photodetector configuration [8]. This phenomenon is associated with the formation of zinc, tellurium, and cadmium oxides in the course of the CdS film sputtering on the film surface of solid solution $\text{Cd}_x\text{Zn}_{1-x}\text{Te}$.

3.4. On the mechanism of injection photocurrent enhancement in the cascade injection photodetector

Our experiments showed that the $\text{In-}n\text{-CdS-}i\text{-CdS}_x\text{Te}_{1-x}\text{-}p\text{-Cd}_x\text{Zn}_{1-x}\text{Te-}p\text{-CdTe-Mo}$ structure manifests itself as an effective injection photodiode at low light illumination levels. In particular, this can be confirmed by current-voltage characteristics measured in dark and under the illuminance $E = 0.5 \div 50$ lux at the temperature $T = 300$ K (see Fig. 4 and Table). To illuminate the structure, we used an incandescent lamp with the power $P = 100$ W. One lumen corresponds to the power of electromagnetic radiation in the visible spectral range equal to 9.1×10^{-3} W [9]. According to the data in Table, the highest integral sensitivity $S_{\text{int}} = 75$ A/lm (about 8×10^3 A/W) is reached at the illuminance $E = 0.5$ lux. The sensitivity decreases, as the illuminance E grows, and becomes equal to 3 A/lm (about 3.4×10^2 A/W) at $E = 50$ lux.

The mechanisms of injection photocurrent enhancement were discussed in work [1]. The operation principle of the injection photodetector created by us is based on the drift transfer of charge carriers. Therefore, the conductance of its base is governed by injected carriers and nonequilibrium carriers generated by electromagnetic radiation. As a result, the injection enhancement is directly connected with the modulation of the base conductance and the conductances of other layers in the photodetector structure. Hence, the mechanism of photocurrent amplification

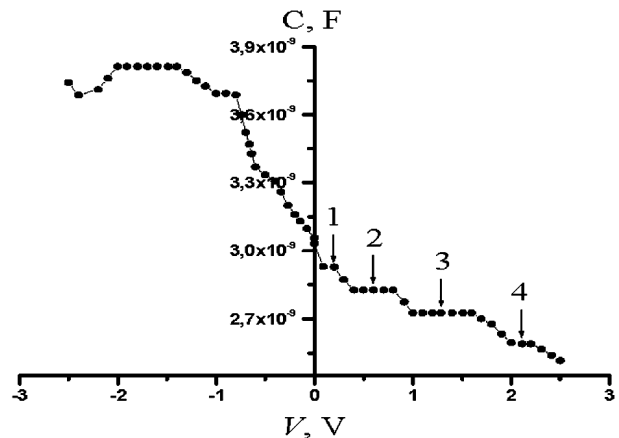


Fig. 3. Capacity-voltage characteristic of the typical $\text{In-}n\text{-CdS-}i\text{-CdS}_x\text{Te}_{1-x}\text{-}p\text{-Cd}_x\text{Zn}_{1-x}\text{Te-}p\text{-CdTe-Mo}$ structure measured at room temperature and the frequency $f = 5$ kHz

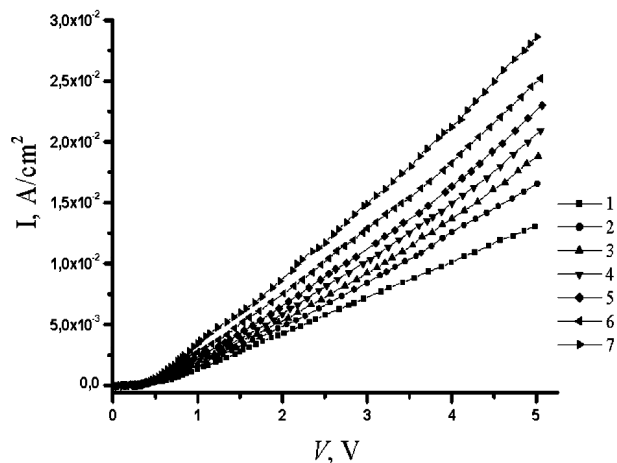


Fig. 4. Dark (1) and light current-voltage characteristics of the typical In-n-CdS-i-CdS_xTe_{1-x}-p-Cd_xZn_{1-x}Te-p-CdTe-Mo structure at various illumination levels of 0.5 (2), 2.5 (3), 7.5 (4), 15 (5), 30 (6), and 50 lux (7) measured at room temperature

is based on a positive feedback that provides the photoconductivity growth and the high integral sensitivity of the developed CIPD at room temperature.

In order to determine the contribution of CdTe layers with hexagonal and cubic modifications to the structure base resistance, the current-voltage characteristic of the structure under the radiation emitted by a laser with $\lambda = 0.625 \mu\text{m}$ and the power $P = 12.5 \text{ mW}$ was studied. The spectral sensitivity of the structure was found to equal $S_\lambda = 0.64 \text{ A/W}$, which is comparable with the spectral sensitivity of

Integral sensitivity of In-n-CdS-i-CdS_xTe_{1-x}-p-Cd_xZn_{1-x}Te-p-CdTe-Mo structure for the forward current direction at various low levels of illumination. The bias voltage $V_b = 5 \text{ V}$ and the temperature $T = 300 \text{ K}$. Notation: V_b is the bias voltage, E the illuminance, I_{dark} the dark current, I_{photo} the photocurrent, and S_{int} the integral sensitivity for the forward current direction

$V_b, \text{ V}$	$E, \text{ lux}$	$I_{\text{dark}}, \text{ mA}$	$I_{\text{photo}}, \text{ mA}$	$S_{\text{int}}, \text{ A/lm}$
5.0	0.0	6.535		
	0.5		8.25	73
	2.5		9.4	23
	7.5		10.3	10.12
	15		11.5	6.35
	30		12.6	4.05
	50		14.3	3.12

ideal photodetectors on the basis of hexagonal ($\approx 0.65 \text{ A/W}$, $\lambda = 0.82 \mu\text{m}$) and cubic ($\approx 0.7 \text{ A/W}$, $\lambda = 0.87 \mu\text{m}$) cadmium telluride [10]. By analyzing the experimental data, we come to a conclusion that the resistances of CdTe layers are modulated by laser radiation; however, their contribution to the total resistance of the structure base is insignificant. It is also follows that the contribution of five interlayers of solid solution Cd_xZn_{1-x}Te with different energy gap widths $E_g \approx 1.89 \div 1.587 \text{ eV}$ to the total resistance of the base is not substantial. It is so because the magnitude $S_{\text{int}} = 75 \text{ A/lm}$ ($\approx 8 \times 10^3 \text{ A/W}$) obtained at the illuminance $E = 0.5 \text{ lux}$ and the value $S_{\text{int}} \approx 0.64 \text{ A/W}$ obtained at the action of laser radiation differ from each other by more than four orders of magnitude.

Therefore, in order to create specimens of film CIPD with the spectral interval of sensitivity extended into the near infra-red region ($\lambda \approx 0.5 \div 0.825 \mu\text{m}$), the photosensitivities of the CdTe layer and the intermediate layers of solid solution Cd_xZn_{1-x}Te adjacent to it must be enhanced. The injection amplification in those layers can be achieved by compensating them with impurities in order to induce a large resistance, which will additionally stimulate a strong modulation of the total resistance of the whole structure.

4. Conclusions

To summarize, the following conclusions can be drawn up.

1. The cascade injection photodetector created on the basis of A²B⁶ compounds effectively works in a wide spectral range, including the far ultraviolet and visible regions, $\lambda \approx 0.5 \div 0.65 \mu\text{m}$. In the whole indicated wavelength interval, its photosensitivity is a few (2 to 3) orders of magnitude higher than the sensitivity of single-crystalline A²B⁶-based injection photodetectors (ZnS-IPDs), which effectively operate only in a narrow ultra-violet interval $\lambda \approx 0.3 \mu\text{m}$.

2. Injection enhancement of the photocurrent in film CIPDs arises owing to the penetration of radiation-generated charge carriers into the base depth due to the action of an external electric field and, as a result, a strong modulation of the base resistance. The high values of the photosensitivity and injection enhancement coefficients in the examined spectral interval follow from the peculiarities in the structure of those CIPDs, where the film of A²B⁶

semiconductors and films of their solid solutions with a varying composition content are used. The presence of layers with different contents, specific resistances, and energy gap widths (for the latter, the difference is $\Delta E = (2.48-1.45) \text{ eV} \approx 1.022 \text{ eV}$) in the photodetector structure brings about the emergence of a built-in electric field E_v . This field promotes an additional penetration of those charge carriers that could be captured by traps into the base. The indicated circumstances allow the resistance of structure base to be effectively modulated and CIPDs with a high integral sensitivity $S_{\text{int}} = 75 \text{ A/lm}$ ($\approx 8 \times 10^3 \text{ A/W}$) to be created on the basis of this structure.

3. It is of importance that the spectral range of the photosensitivity was expanded owing to the creation of an energy-gap gradient, $\text{grad}(\Delta E_g)$, in the photodetector structure. As a result, quanta of different energies are effectively absorbed in certain layers of the CIPD sensitive region, and the resistance of those layers can be modulated.

4. An important advantage of the created CIPD consists in that it operates in the forward direction and is capable of registering and effectively enhancing the weak optical signals at the illuminance level not lower than $E = 0.5 \div 50 \text{ lux}$ in the indicated spectral interval and at room temperature.

The operational parameters of CIPD, such as wide spectral interval, low V_b value, high integral sensitivity, and capability to work effectively at the temperature $T = 300 \text{ K}$, when comparing them with the corresponding characteristics of other solid-state photodetectors, testify that photodetectors of this type will find practical applications in various devices for the registration and the analysis of optical signals in the visible spectral range.

1. I.M. Vikulin, Sh.D. Kurmashev, and V.I. Stafeev, *Fiz. Tekh. Poluprovodn.* **42**, 113 (2008).

2. Sh.A. Mirsagatov and A.K. Uteniyazov, *Pis'ma Zh. Tekhn. Fiz.* **38**, No. 1, 70 (2012).
3. N.V. Parol and S.A. Kaidalov, *Photosensitive Devices and Their Application* (Radio i Svyaz, Moscow, 1991) (in Russian).
4. *Semiconductors and Semimetals. Vol. 3. Optical Properties of III-V Compounds*, edited by R.K. Willardson and A.C. Beer (Academic Press, New York, 1967).
5. E.B. Zaveryukhina, and B.N. Zaveryukhin, N.N. Zaveryukhina, *Pis'ma Zh. Tekhn. Fiz.* **33**, No. 9, 1 (2007).
6. Sh.A. Alimov, V.V. Losev, B.M. Orlov, and V.I. Stafeev, *Fiz. Tekh. Poluprovodn.* **10**, 1830 (1976).
7. K. Zanio, *Semiconductors and Semimetals* (Academic Press, New York, 1978).
8. S.M. Sze, *Physics of Semiconductor Devices* (Wiley, New York, 1981).
9. S.E. Frish, *Optical Measurement Methods. Part 1: Light Flux and Its Measurement; Light Sources* (Leningrad University Publ. House, Leningrad, 1976) (in Russian).
10. A. Ambroziak, *Konstrukcja i Technologia Przyrządów Fotoelektrycznych* (Wyd. Nauk.-Techn., Warszawa, 1967).

Received 12.06.12.

Translated from Ukrainian by O.I. Voitenko

*Ш.А. Мірсагатов, Б.Н. Заверюхін,
О.К. Атабов, М.М. Заверюхіна*

КАСКАДНИЙ ІНЖЕКЦІЙНИЙ ФОТОПРИЙМАЧ
НА ОСНОВІ ТВЕРДИХ РОЗЧИНІВ А²В⁶-СПОЛУК
ДЛЯ СПЕКТРАЛЬНОГО ДІАПАЗОНУ $\lambda = 500-650 \text{ нм}$

Резюме

Створено та досліджено плівковий інжекційний фотоприймач (ПФП) на основі твердих розчинів А²В⁶-сполук для спектрального діапазону $\lambda \approx 0,5-0,65 \text{ мкм}$. Чутлива область ПФП сформована у вигляді сендвіча з плівок змінного складу і з різними ширинами заборонених зон. Механізм роботи ПФП заснований на селективному поглинанні спектра випромінювання плівками і перетворенні його в електричний сигнал. ПФП мають внутрішнє підсилення фотоструму і ефективно реєструють слабкі оптичні сигнали при освітленості $E \leq 1 \text{ лк}$ і $T = 300 \text{ К}$. Інтегральна чутливість ПФП $S_{\text{int}} \approx 75 \text{ А/лм}$ ($\approx 8 \cdot 10^3 \text{ А/Вт}$).